FLEXURAL STRENGTHENING OF REINFORCED LOW STRENGTH CONCRETE SLABS USING PRESTRESSED NSM CFRP LAMINATES

M. R. Mostakhdemin Hosseini[1], S. J. E. Dias[2] and J. A. O. Barros[3]

[1] Phd Student, ISISE, Dep. of Civil Eng., Univ. of Minho, Azurém, 4810-058 Guimarães, Portugal

[2] Assistant Prof., ISISE, Dep. of Civil Eng., Univ. of Minho, Azurém, 4810-058 Guimarães, Portugal

[3] Full Prof., ISISE, Dep. of Civil Eng., Univ. of Minho, Azurém, 4810-058 Guimarães, Portugal

ABSTRACT

The effectiveness of the Near Surface Mounted (NSM) technique with prestressed CFRP (carbon fiber reinforced polymer) laminates for the flexural strengthening of reinforced concrete (RC) slabs of low strength concrete was assessed. Four RC slabs were tested, a reference slab (without CFRP), and three slabs flexurally strengthened using NSM CFRP laminates with different prestress level of the ultimate tensile strength of the CFRP: 0%, 20% and 40%. The experimental program is described and the main results are presented and analyzed in terms of the structural behavior of the RC slabs, failure modes and performance of the NSM technique with prestressed CFRP laminates. The results show that prestressing CFRP laminates with NSM technique is an effective technology to increase cracking, service, yielding and maximum loads of RC slabs made by low strength concrete. By applying NSM CFRP laminates prestressed at 20%, the cracking, service and maximum loads have increased, respectively, 258%, 123% and 125%, when the corresponding values of the reference slab are taken for comparison purposes, while 400%, 190% and 134% were the increase when applying laminates prestressed at 40%. Using available experimental results obtained with the same test setup, but using RC slabs of higher strength concrete, it can be concluded that as minimum is the concrete strength as more effective is the NSM technique with prestressed CFRP laminates in terms of serviceability limit states. A numerical strategy was used to evaluate the load-deflection of the tested RC slabs and to highlight the influence of the percentage of CFRP, the percentage of tensile longitudinal bars and the elasticity modulus of the CFRP on the effectiveness of the NSM technique with prestressed CFRP laminates for the flexural strengthening of RC slabs, by performing a parametric study.

KEYWORDS: A. Carbon fibre; B. Strength; C. Numerical analysis; D. Mechanical testing; Prestressed NSM CFRP laminates

1. INTRODUCTION

Using carbon fiber reinforced polymers (CFRP), competitive structural strengthening solutions can be developed due to the high strength-to-weight and stiffness-to-weight ratios, high durability (non corrodible), electromagnetic neutrality, ease of handling, rapid execution with low labor, and practically unlimited availability in size, geometry and dimension of these advanced materials [1-3].

For flexurally strengthening of reinforced concrete (RC) structural elements, CFRP materials can be applied according to the followings two main techniques: bonding wet lay-up sheets or laminates to the external tension faces of the elements to be strengthened (Externally Bonded Reinforcement - EBR - technique) [4-6]; installing CFRP bars (circular, square or rectangular cross section) into pre-cut slits opened on the concrete cover of the elements to strengthen (Near Surface Mounted - NSM - technique) [6-10]. Due to the largest bond area and higher confinement provided by the surrounding concrete, narrow strips of CFRP laminates of rectangular cross section, installed into thin slits and bonded to concrete by an epoxy adhesive, are the most effective CFRP strengthening elements for the NSM technique [8].

The efficacy of the NSM strengthening technique with passive CFRP laminates to increase the flexural resistance of RC beams [6-10] and slabs [11-12] was already well assessed. In fact, NSM CFRP laminates without any prestress level can increase significantly the ultimate load carrying capacity of RC structural elements, and high mobilization of the tensile properties of the CFRP can be assured. However, for deflection levels corresponding to the serviceability limit states the benefits of the CFRP are, in general, of small relevance. By prestressing the CFRP, its high tensile capacity is more effectively used, contributing to increase significantly the load carrying capacity of the strengthened elements under both service and ultimate conditions. The prestress can also contribute to close eventual existing cracks, to decrease the tensile stress installed in the existing flexural reinforcement, and to increase the shear capacity of these elements. Thus, prestressing the CFRP seems to be a cost-effective solution to increase both the structural performance and the durability of the strengthened RC structure.

Recent experimental research has demonstrated that applying NSM CFRP laminates with a certain prestress level for the flexural strengthening of RC beams [13-16] and slabs [17] can mobilize better the potentialities of these high tensile strength materials, with an appreciable increase of the load carrying capacity at serviceability and ultimate limit states.

There are several reasons that justify the relevance of a study on the use of the NSM technique with prestressed CFRP laminates for the flexural strengthening of RC slabs of low strength concrete: old RC structures were built with low strength concrete; decrease of concrete strength due to several time dependent phenomena and environmental conditions; evaluate the role of the concrete in the effectiveness of this highly effective technique.

To appraise the potentialities of applying NSM prestressed CFRP laminates for the flexural strengthening of low strength concrete slabs, an experimental program was carried out. The average value of the concrete compressive strength at the age of the slabs tests was 15.0 MPa. The experimental program is outlined and the specimens, materials and test setup are described. The results of the tests are presented and discussed and a number of conclusions are drawn. Taking the results obtained in a previous experimental program [17], characterized by the same test setup, but using RC slabs of higher concrete strength (46.7 MPa instead of 15.0 MPa), the influence of the concrete mechanical properties in the performance of the NSM technique with prestressed CFRP laminates for the flexural strengthening of RC slabs was assessed.

A numerical strategy was used to evaluate the load-deflection of the tested RC slabs, and a comparison between experimental and numerical results was done. This numerical strategy was adopted to execute a parametric study in order to evaluate the influence of the percentage of CFRP, the percentage of tensile longitudinal bars and the elasticity modulus of the CFRP on the effectiveness of the NSM technique with prestressed CFRP laminates for the flexural strengthening of RC slabs.

2. EXPERIMENTAL PROGRAM

2.1. Test series

The experimental program is composed of four RC slabs with a rectangular cross section of 120×600 mm^2, a total length of 2600 mm and a span length of 2400 mm. The longitudinal steel reinforcement consisted of 3 bars of 6 mm diameter (3ϕ6) in the compression zone and 4 bars of 8 mm diameter (4ϕ8) in the tension zone. Steel stirrups of 6 mm diameter spaced at 300 mm (ϕ6@300mm) are adopted as transversal reinforcement, and have the main purpose of maintaining the longitudinal reinforcement in the aimed position. The adopted reinforcement systems were designed to assure flexural failure mode for all the tested slabs. Fig. 1 represents the cross section geometry and the reinforcement arrangement for each slab, as well as the longitudinal geometry, loading configuration and support conditions. The concrete clear cover of the longitudinal tensile bars was 31 mm.

The general information of the four tested RC slabs is represented in Table 1. The SREF is the reference slab without CFRP, and the S2L-0, S2L-20 and S2L-40 slabs are those flexurally strengthened using two NSM CFRP laminates (Fig. 2) with different prestress level: 0% (S2L-0), 20% (S2L-20) and 40% (S2L-40) of the ultimate tensile strength of the CFRP laminates. The CFRP laminates used in the present experimental program have a cross section of 1.4 (thickness)×20 (depth) mm^2. Table 1 shows that the tested slabs have a percentage of longitudinal tensile steel bars (ρ_{sl}) of about 0.39%, while the CFRP strengthening percentage (ρ_f) is approximately 0.08%.

The four point slab bending tests (Fig. 3) were executed under displacement control at a deflection rate of 0.02 mm/second. All slabs were instrumented to measure the applied load, deflections and strains in the CFRP laminates and longitudinal tensile steel reinforcement. Positions of the LVDTs (linear variable displacement transducers) and strain gauges (SG) in the monitored longitudinal tensile bars and in the NSM CFRP laminates are indicated in Fig. 4. The deflection of the slabs was measured by five displacement transducers (LVDT 1 to LVDT 5) according to the arrangement indicated in Fig. 4a. To evaluate the strains on the steel bars, two strain gauges were installed (Fig. 4b) on the two bottom longitudinal steel bars (SG-S1 and SG-S2). In the non-prestressed slab (S2L-0), three strain gauges were installed on the two CFRP laminates (SG-L1 to SG-L3) according to the scheme represented in Fig. 4c, while in the prestressed slabs (S2L-20 and S2L-40) the disposition of the six strain gauges (SG-L1 to SG-L6) applied on the two CFRP laminates is indicated in Fig. 4d (the SG-L4 to SG-L6 strain gauges were installed near the end of the CFRP laminates to determine prestress losses).

According to Fig. 4c, the length of the laminates in S2L-0 slab was 2300 mm. For the RC slabs flexurally strengthened with prestressed laminates the slits were executed along the total length of the slab, but the extremities of the laminates were not bonded to the concrete in a length of 150 mm in order to provide the same bond length adopted in the S2L-0 slab.

2.2. Materials properties

The compressive strength [18] and Young's modulus [19] of the concrete were evaluated at the age of the slab tests (336 days) carrying out direct compression tests with cylinders of 150 mm diameter and 300 mm height. The values of the main tensile properties of the high bond steel bars (6 and 8 mm diameter) used in the tested slabs were obtained from uniaxial tensile tests performed according to the recommendations of EN 10002 [20]. The tensile properties of the CFK 150/2000 S&P laminates were characterized by uniaxial tensile tests carried out according to ISO 527-5 [21]. Table 2 includes the average values obtained from these experimental programs.

S&P Resin 220 epoxy adhesive was used to bond the CFRP laminates to the concrete substrate. The instantaneous and long term tensile behavior of this adhesive was investigated by Costa and Barros [22]. At 3 days, at which the elasticity modulus ($\boldsymbol{E_{0.5\sim2.5‰}}$) has attained a stabilized value, the tensile strength and the $\boldsymbol{E_{0.5\sim2.5‰}}$, determined according to the ISO 527-2 recommendations [23] was about 20 MPa and 7 GPa, respectively.

2.3. Application of the NSM CFRP laminates

To apply the passive CFRP laminates using NSM technique, the following procedures were executed: 1) using a diamond cutter, slits of about 5 mm width and 25 mm depth were opened on the concrete cover of the tension face according to the pre-defined arrangement for the laminates; 2) the slits were cleaned by compressed air; 3) the laminates were cut with the desired length and cleaned with acetone; 4) the epoxy adhesive was produced according to the supplier recommendations; 5) the slits were filled with the adhesive; 6) an adhesive layer was applied on the faces of the laminates; and 7) the laminates were inserted into the slits and adhesive in excess was removed.

Fig. 5 shows the device for applying the prestressing force to the laminates, which includes the main system to apply the pressure into the hoses, handle for controlling the oil pressure, hydraulic hollow jacks for transferring force to the laminates and load cells that were installed between hydraulic jacks and main frame to control the value of prestressing load. To ensure that the release of the prestress force would occur simultaneously in both extremities of the RC slabs, two steel rollers were placed under the slabs. The design details of the mechanical components of this prestressing system can be consulted elsewhere [24]. After installing the slab in the right position of prestressing line, the CFRP laminates were placed into the slits and passed through the hydraulic jacks and load cells, and were anchored in both extremities by using an active and a passive anchor, as is shown in the Fig. 5. Each laminate was installed in the middle of the slit, as closest as possible to the slab's external surface, and then the prestressing force was applied.

In S2L-20 and S2L-40 slabs the prestressing load for each laminate was about, respectively, 20% and 40% of the laminate ultimate tensile strength. The prestressing force was applied to one extremity of the laminate by the hydraulic jack (active anchor), while the other extremity of the CFRP laminate remained fixed to the main frame of prestress line by using steel anchors (passive anchor). The increase of the prestressing load was about 0.5 kN/min. When the prestressing load was completely applied to the laminates, epoxy adhesive was applied into the slits by using a spatula, as shown in Fig. 5. Special care was taken in the execution of this task in order to avoid the formation of voids in the concrete-adhesive-CFRP interfaces, as well as into the adhesive layer. After about six days of the application of the adhesive, the prestressing load was released slowly and simultaneously in both CFRP laminates at a load rate of about 0.3 kN/min.

Fig. 6a shows the variations of strains on the CFRP laminates during less than one day after releasing the prestressing loads on the prestressed strengthened slabs. Fig. 6b shows the variations of strains on the CFRP laminates during one week after releasing the prestressing loads on the prestressed strengthened slabs. Table 3 shows the decrease of strains (in terms of percentage of the initial prestress strain) during one week after releasing the prestress on the CFRP laminates. This decrease is due to the loss of prestress in consequence of the deformability of the adhesive layer, concrete deformability and eventual sliding at concrete-adhesive-laminate interfaces. As this table shows, when the prestressing loads were released, the strain gauge closest to the free extremity of the laminate (SG-L6, that was at a distance of 25 mm far from this extremity - see Fig. 4) recorded after seven days a strain loss of about 48.2% and 50.1% in the S2L-20 and S2L-40 slabs, respectively (after 24 hours the strain loss in this SG was 38.7% and 47.1%, respectively). After seven days, the rest of the strain gauges showed a loss of strain less than 9% and 13% for the S2L-20 and S2L-40 slabs, respectively, which indicated that the main part of the prestressing load was transferred to the concrete slab as expected.

3. EXPERIMENTAL RESULTS AND DISCUSSION

3.1. Load carrying capacity of the tested slabs

Fig. 7 shows the relationship between the applied force and the deflection at mid-span, *F-u*, for the four tested RC slabs. This figure shows that the experimental load-displacement curves of the slabs have three important phases: up to concrete cracking; between concrete cracking and yield initiation of the steel reinforcement; and between steel yield initiation and ultimate load. As expected, the unstrengthened control slab behaved in a plastic manner in the third phase. The almost linear slop of the third phase of strengthened slabs is due to the contribution of the CFRP, since the laminates have linear behavior, while steel reinforcement is in a plastic stage and cracked concrete is too damaged. In fact, above the deflection corresponding to yield initiation, the load carrying capacity of the strengthened slabs has increased up to the CFRP rupture, after which the load dropped to that of the control slab. Regardless the prestress level of the laminates (0%, 20% and 40%), the adopted CFRP configuration provided an increase in the slab's load carrying capacity at serviceability and ultimate limit states.

Table 4 shows the summary of the results of the tested RC slabs in terms of cracking (F_{crack}), service ($F_{serv.}$), yielding (F_{sy}) and maximum (F_{max}) load (see also Fig.7). The values of the deflection at mid-span for the loads F_{sy} ($u_{Fsy.}$) and F_{max} (u_{Fmax}) are also indicated in Table 4. The service load (F_{serv}) is the load corresponding to the maximum allowed deflection for serviceability limit states (u_{Fserv}), which according to the Eurocode 2 [25] is *l/250*, where *l* is the slab span length (*l*/250 = 2400 mm/250 = 9.6 mm). The yielding load is herein defined as the load at which a considerable decay of stiffness has occurred (see Fig. 7).

Strengthening the RC slabs with NSM CFRP laminates resulted in higher cracking loads than the F_{crack} of the reference slab. The F_{crack} has increased with the prestress level (the values of F_{crack} of reference, non-prestressed, 20% and 40% prestressed slabs are respectively, 3.1 kN, 4.2 kN, 11.1 kN and 15.5 kN). Based on Table 4, the values of service load of reference, non-prestressed, 20% and 40% prestressed slabs are respectively, 9.2 kN, 13.1 kN, 20.54 kN and 26.7 kN, which evidence the benefits of applying the CFRP laminates with a certain prestress. Strengthening the RC slabs with NSM CFRP laminates resulted also in higher yielding loads than the F_{sy} of the reference slab. The F_{sy} has increased with the prestress level. The values of maximum load of strengthened slabs ranged between 51.11 kN and 55.65 kN, which is 2.2 and 2.3 times higher the maximum load of the reference slab (23.75 kN).

Since the load at crack initiation increases with the prestress level, and considering the stiffness and load amplitude between crack initiation and yield initiation do not change significantly with the prestress level, the deflection at yield initiation do not change significantly with the increase of the prestress level. By increasing the prestress level, larger initial strains are introduced in the CFRP laminates. Due to this fact and considering the CFRP has ruptured at maximum load, the corresponding slab's deflection has decreased with the prestress level.

3.2. Crack pattern and failure modes

Fig. 8 shows the final crack pattern of the tested RC slabs. By strengthening RC slabs with NSM CFRP laminates, the average distance between cracks decreased. In fact the values of the average distance between cracks are 126 mm, 101 mm, 86 mm and 79 mm, respectively for the slabs SREF, S2L-0, S2L-20 and S2L-40. During the tests of the RC slabs until the failure it was possible to observe that the crack width have decreased by strengthening RC slabs with NSM CFRP laminates. When the final crack pattern of the NSM slabs is compared, it is possible to conclude that the length of the slab's cracked band has decreased with the increase of the prestress level due to the initial compressive strain field introduced by the prestress. In fact the values of the slab's cracked band are 1639 mm, 1826 mm, 1550 mm and 1260 mm, respectively for the slabs SREF, S2L-0, S2L-20 and S2L-40.

Two types of failure modes occurred in the tested RC slabs: 1) the reference slab failed by the concrete crushing after the yielding of the tensile steel reinforcements (see Fig. 9a). In this slab, at mid-span deflection of 143 mm (Fig. 7) a longitudinal steel bar has ruptured (see Fig. 9a); 2) the strengthened slabs failed by the rupture of the CFRP (see Fig. 9b) after the yielding of the tensile steel reinforcements.

3.3. Strains in CFRP laminates and tensile steel reinforcements

The maximum strain values recorded in the strain gauges installed in the CFRP laminates up to the maximum load (F_{max}) of the slabs are indicated in the column "Total" of the Table 5. Each of these values is the addition of the strain at the end of the prestress phase (column "Prestressing") with the maximum strain registered in the loading phase of the slab up to its F_{max} (column "Test"). The maximum values of strain measured in the CFRP laminates (column "Total"), namely in the SG-L2, are quite close to the ultimate tensile strain of the CFRP, justifying the failure mode of the strengthened slabs and the high effectiveness of the NSM technique for the flexural strengthening of RC slabs. Based on this table, by increasing the level of prestress, the total strain in the CFRP laminates has increased, which shows that by increasing the level of prestress the probability of using more capacity of CFRP laminates increase.

Fig. 10a shows the relationship between the applied load and the strain in the SG-L2 strain gauge (Fig. 4). The initial strain of CFRP laminates in 0%, 20% and 40% prestressed slabs are, respectively, 0‰, 3.16‰ and 5.92‰, as also indicated in Table 5. According to the Fig. 10a, the load-CFRP strain curves of the slabs have a common configuration formed by the three phases already mentioned in the analysis of the Fig. 7: 1) until concrete cracking with an almost null variation; 2) between concrete cracking and yield initiation of the steel reinforcement, where the strain has increased with the load; 3) and between steel yield initiation and ultimate load, with an almost equal strain gradient in all the slabs, which is much more pronounced than in the previous phase, due to the plastic stage of the steel reinforcement.

Fig. 10b presents the relationship between the applied load and strain in the longitudinal tensile steel reinforcement (SG-S2 in Fig.4). Based on this figure, the tensile steel reinforcement in the prestressed slabs (S2L-20 and S2L-40) presented initial compressive strains before the application of external loading due to the prestress force transferred from the laminates for the surrounding concrete. During the external loading process these steel bars started to present tensile strains. The load that converts strain on the tensile steel reinforcements from compression to tension is defined as decompression load, as indicated in Fig. 10b. In the prestressed slabs, the yielding of steel reinforcements occurred at higher load levels (F_{sy}) due to the initial compressive strains introduced by the prestress effect of the CFRP laminates. According to Fig. 10b the steel decompression load has increased with the prestress level, and consequently the yielding load (F_{sy}) of slabs has increased (as mentioned in Table 4).

3.4. Effect of the prestress

To evaluate the effect of the prestress level of CFRP laminates on the overall flexural behavior of RC slabs, the values of forces (F_{cr}^{Str} , F_{serv}^{Str}, F_{max}^{Str}) and corresponding deflection to F_{max}^{Str} ($u_{F_{max}}^{Str}$) of the strengthened prestressed slabs are compared in Table 6 with those corresponding values of the reference slab (F_{cr}^{Ref} , F_{serv}^{Ref} , F_{max}^{Ref} , $u_{F_{max}}^{Ref}$). By considering these values, the parameters $\Delta F_{cr}/F_{cr}^{Ref}$, $\Delta F_{serv}/F_{ser}^{Ref}$, $\Delta F_{max}/F_{max}^{Ref}$, $\Delta u_{F_{max}}/u_{F_{max}}^{Ref}$ were evaluated and included in Table 6, where $\Delta F_{cr} = F_{cr}^{Str} - F_{cr}^{Ref}$, $\Delta F_{serv} = F_{serv}^{Str} - F_{ser}^{Ref}$, $\Delta F_{max} = F_{max}^{Str} - F_{max}^{Ref}$ and $\Delta u_{F_{max}} = u_{F_{max}}^{Str} - u_{F_{max}}^{Ref}$.

The obtained results evidence that applying a prestress level of 0%, 20% and 40% in the CFRP laminates has provided an increase of, respectively, 35%, 258% and 400% in cracking load, an increase of, respectively, 42%, 123% and 190% in service load, and an increase of, respectively, 115%, 125% and 134% in maximum load. However, the maximum deflection has increased in 20% for the prestress level of 0%, while it has decreased in 9% and 31% by applying a prestress level of, respectively, 20% and 40%. Nonetheless, at u_{Fmax} both the prestressed slabs had already experienced a large incursion on the plastic stage of the steel reinforcement, therefore the level of ductility is still significantly high in the prestressed slabs.

Fig. 11 shows the effect of increasing the prestress level on the cracking, service, yielding and ultimate loads with respect to the corresponding load values in the reference slab, SREF, and in the non-prestressed strengthened slab, S2L-0. This figure clearly evidences the pronounced favorable effect of the prestress level in terms of load carrying capacity of RC slabs at cracking, serviceability and at yield initiation stages, while the increase of ultimate load was not significantly affected by the prestress level adopted.

Fig. 12 represents the effect of increasing the prestress level on the deflection at yielding and ultimate loads. When compared to the corresponding values recorded in the SREF and S2L-0 slabs, it is verified a significant decrease of ultimate deflection with the increase of the prestress level, but the yielding deflection was not considerably affected by the prestress level.

Fig. 13 shows the relation between the prestressing level and the normalized value of energy consumed during the loading process of the slabs up to the u_{Fmax}. This energy concept was calculated for each tested RC slab as the area under the load-deflection curve. The above mentioned normalized value of energy is the ratio between the energy of the strengthened RC slab and the energy of the reference RC slab. It is observed an almost linear decrease of the energy consumed with the increase of the prestress level. However, regardless of level of prestress, the energy absorption of the strengthened RC slabs was significantly higher than the one of the reference slab.

4. INFLUENCE OF THE CONCRETE STRENGTH ON THE EFFECTIVENESS OF THE NSM TECHNIQUE WITH PRESTRESSED CFRP LAMINATES

In the present section the influence of concrete strength on the efficacy of the NSM technique with prestressed CFRP laminates is assessed comparing the results of the experimental program described in previous sections with the results of other experimental program [17] dealing with RC slabs of higher concrete strength. In the experimental program described in [17] the geometry of RC slabs, arrangement of NSM CFRP laminates, loading configuration and support conditions presented in Fig. 2 were the same adopted in the present experimental program, but the RC slabs were manufactured with a concrete of a compressive strength at the testing age of the slabs of 46.7 MPa (f_{cm} = 46.7 MPa instead of f_{cm} = 15.0 MPa - see Table 2). In both experimental programs, the percentage of the steel reinforcement is similar, and the applied prestressed levels were the same.

To evaluate the effect of concrete strength on the efficacy of the NSM technique with prestressed CFRP laminates, for both experimental programs above mentioned (one where the concrete has f_{cm} = 15.0 MPa and the other where the concrete has f_{cm} = 46.7 MPa) the values of forces (F_{serv}^{Str}, F_{max}^{Str}) and deflection corresponding to F_{max}^{Str} ($u_{F_{max}}^{Str}$) of the strengthened prestressed slabs are compared with those values of the reference slab (F_{serv}^{Ref}, F_{max}^{Ref}, $u_{F_{max}}^{Ref}$). By considering these values, the parameters $\Delta F_{serv}/F_{ser}^{Ref}$, $\Delta F_{max}/F_{max}^{Ref}$, $\Delta u_{F_{max}}/u_{F_{max}}^{Ref}$ were evaluated for the RC slabs of the above mentioned experimental programs ($\Delta F_{serv} = F_{serv}^{Str} - F_{ser}^{Ref}$, $\Delta F_{max} = F_{max}^{Str} - F_{max}^{Ref}$ and $\Delta u_{F_{max}} = u_{F_{max}}^{Str} - u_{F_{max}}^{Ref}$), and the obtained results are included in Table 7.

According to these results, regardless the concrete quality, by increasing the prestress level in the NSM CFRP laminates, the overall flexural behavior of the slabs at service and ultimate stages has improved (Fig. 14), but the deflection at the maximum load has decreased with the increase of the prestress level. By applying 20% of prestress in the NSM CFRP laminates of slabs with higher and lower concrete compressive strength, the service load has increased, respectively, 55% and 123% when compared to the corresponding values of the reference slab, while 40% of prestress has guaranteed an increase of 119% and 190%, respectively. The higher strengthening efficiency of the prestressed NSM CFRP laminates in the slabs with the lower concrete is caused by the higher increase registered in terms of cracking load. By applying 20% of prestress in the NSM CFRP laminates of slabs with higher and lower concrete compressive strength, the ultimate load has increased, respectively, 136% and 125% when compared to the corresponding values of the reference slab, while 40% of prestress has guaranteed an increase of 152% and 134%.

5. NUMERICAL SIMULATION AND PARAMETRIC STUDY

5.1. Numerical simulation

Previous work [9] shown that, using a cross section layered model that takes into account the constitutive laws of the intervening materials, and the kinematic and the equilibrium conditions, the deformational behavior of structural elements failing in bending can be predicted from the moment–curvature relation, M–χ, of the representative cross sections of these elements, using the algorithm described elsewhere [26, 27].

To evaluate the M–χ relationship, the slab cross section was discretized in layers of 1 mm thick. To simulate the behavior concrete in compression, the stress-strain relationship recommended by model code CEB-FIP Model Code 90 [28] was used (see Fig. 15a). Concrete was assumed as behaving linearly up to its tensile strength, while in the post-cracking stage the bilinear tension-stiffening diagram, represented in Fig. 15b, considered by Barros and Fortes [9], was used. In this figure, f_{ctm} is the average concrete tensile strength determined from the average compressive strength (f_{cm}) by adopting the Eurocode 2 [25] recommendations. The considered values for the parameters α_1 and ζ_1 were, respectively, 0.55 and 3.

The stress-strain diagram used to model the tension and the compression behavior of steel bars is represented in Fig. 16 [9]. The data defining this relationship is indicated in Table 8. For modeling the tensile behavior of the CFRP laminates, a linear elastic stress-strain relationship was adopted, by using the values indicated in Table 2.

Fig. 17 compares the relationship between the applied load and the deflection at mid-span recorded experimentally and obtained in the numerical simulations. As Fig. 17 shows, the adopted numerical strategy fits with enough accuracy the registered experimental load *vs.* mid-span deflection curves of the tested slabs.

5.2. Parametric study

The numerical strategy, whose good predictive performance for the simulation of the structural behavior of the RC slabs flexurally strengthened using prestressed NSM CFRP laminates was confirmed in the previous section, is now adopted to execute a parametric study for the evaluation of the influence on the load carrying capacity of the following parameters: percentage of the CFRP, percentage of tensile longitudinal bars and the elasticity modulus of the CFRP. In fact, according to Table 9 and Fig. 18, for each of the above mentioned parameters it was analyzed three scenarios (A, B and C). For comparison purposes, the results obtained in the previous section (slabs S2L-20 and S2L-40) were adopted in this parametric study. The geometry of the RC slabs, the arrangement of the steel reinforcement, the material properties of concrete, and the support and load conditions were the same ones adopted in the numerical simulations of the previous section.

The percentage of the CFRP was increased by changing the number of CFRP laminates with a cross section equal to 1.4×20 mm^2 (Fig. 18a): 1 laminate in the scenario A (ρ_f = 0.038%), 2 laminates in the scenario B (ρ_f = 0.077%), and 3 laminates in the scenario C (ρ_f = 0.116%). In Fig. 19 the load-deflection curves for the three different percentage of the CFRP are compared. The values of $\Delta F_{serv}/F_{ser}^{Ref}$ and $\Delta F_{max}/F_{max}^{Ref}$ for the six RC slabs are presented in Table 10 and illustrated in Fig. 20. As expected, by increasing the percentage of the CFRP laminates the overall flexural behavior of the slabs at service and ultimate states has improved. By increasing the prestress level in the NSM CFRP laminates the deflection at the maximum load of the slabs has decreased, regardless the percentage of CFRP laminates adopted.

The percentage of tensile longitudinal bars was increased by changing the diameter of the bars: (Fig. 18b): 4 bars of 8 mm diameter (4ϕ8) (ρ_{sl}= 0.394%) in the scenario A, 4 bars of 10 mm diameter (4ϕ10) (ρ_{sl}= 0.623%) in the scenario B and 4 bars of 12 mm diameter (4ϕ12) (ρ_{sl}= 0.908%) in the scenario C. The relationship between load and deflection at mid-span for the simulated slabs are compared in Fig. 21. As expected, by increasing the percentage of tensile longitudinal bars the overall flexural behavior of the slabs at service and ultimate states has improved (Table 11). The values of $\Delta F_{serv}/F_{ser}^{Ref}$ and $\Delta F_{max}/F_{max}^{Ref}$ for the above mentioned six RC slabs are presented in Table 11 and illustrated in Fig. 22, where it is possible to see that the increase of the percentage of existing tensile longitudinal steel bars has a detrimental effect on the NSM technique with prestressed CFRP laminates for the flexural strengthening of RC slabs, regardless the prestress level of the laminates. By increasing the prestress level in the NSM CFRP laminates the deflection at the maximum load of the slabs has decreased, regardless the percentage of tensile longitudinal bars.

Three values of the elasticity modulus of the FRP laminates were tested (125 GPa, 175 GPa and 225 GPa). The relationship between load and deflection at mid-span for the simulated slabs are compared in Fig. 23. The values of $\Delta F_{serv}/F_{ser}^{Ref}$ and $\Delta F_{max}/F_{max}^{Ref}$ for the six RC slabs are presented in Table 12 and illustrated in Fig. 24. As expected, by increasing the values of the elasticity modulus of the FRP laminates the overall flexural behavior of the slabs at service and ultimate states has improved. By increasing the prestress level in the NSM FRP laminates the deflection at the maximum load of the slabs has decreased, regardless the values of the elasticity modulus of the FRP laminates considered. Furthermore, the benefits in terms of load carrying capacity by increasing the elasticity modulus are potentiated when increasing the prestress level applied to the NSM FRP laminates.

6. CONCLUSIONS

By carrying out an experimental program, the effectiveness of NSM technique with prestressed CFRP laminates for the flexural strengthening of RC slabs of low strength concrete (f_{cm} = 15.0 MPa) was assessed. From the obtained experimental results it can be concluded that:

- Regardless the prestress level of the CFRP laminates, the NSM technique with CFRP laminates is highly effective for the flexural strengthening of RC slabs of low strength concrete. In fact, the adopted CFRP flexural strengthening configuration has provided an increase in terms of maximum load that ranged between 115% and 134% of the maximum load of the reference RC slab.
- By strengthening RC slabs of low strength concrete with prestressed NSM CFRP laminates resulted in a significant increase of load carrying capacity at serviceability and ultimate limit states. By applying 20% of prestress in the NSM CFRP laminates, the cracking, service and ultimate loads have increased, respectively, 258%, 123% and 125% when compared to the corresponding values of the reference slab, while 40% of prestress has guaranteed an increase of 400%, 190% and 134%.
- By increasing the prestress level in the NSM CFRP laminates the overall flexural behavior of the slabs at service and ultimate states has improved, but the deflection at the maximum load of the slabs has decreased with the increase of the prestress level. However, the deflection at maximum load was more than 1.9 times the deflection at yield initiation, with a significant plastic incursion on the steel reinforcement, which assures the required level of deflection ductility for this type of RC structures.
- Regardless the prestress level applied to the CFRP laminates, all the strengthened slabs failed by rupture of the laminates after yielding of the tension steel reinforcement. This failure mode proved the high effectiveness of the NSM technique for the flexural strengthening of RC slabs of low strength concrete.

When the same NSM CFRP laminates arrangements were applied in a group of slabs of concrete compressive strength (f_{cm}) equal to 46.7 MPa and in another group of slabs of f_{cm} = 15.0 MPa, the obtained results showed the NSM technique with prestressed CFRP laminates was more effective in the lowest concrete strength class series of slabs, mainly at serviceability limit state conditions.

A numerical strategy was used to evaluate the load-deflection of the tested RC slabs. Using the properties of the intervening materials in the tested slabs, obtained from experimental tests, the relationship between the force and the mid-span deflection recorded in the tested slabs was predicted with high accuracy, revealing that the adopted numerical strategy is appropriate to simulate the behavior of RC slabs strengthened by NSM technique with CFRP laminates with or without prestress. A parametric study for the evaluation of the influence of the percentage of the

CFRP laminates, the percentage of tensile longitudinal bars and the elasticity modulus of the FRP on the behavior of RC slabs strengthened with prestressed NSM CFRP laminates was also carried out. The results indicated that by increasing each above mentioned parameters, the load carrying capacity of the slabs at service and ultimate states has increased, mainly when increasing the prestress level in the NSM FRP laminates, but the deflection corresponding to the maximum load of the slabs has decreased. Furthermore, the increase of the percentage of tensile longitudinal bars has a detrimental effect on the effectiveness of NSM technique with prestressed CFRP laminates.

Acknowledgements

The authors wish to acknowledge the support provided by the "Empreiteiros Casais" and S&P®. This work was supported by FEDER funds through the Operational Program for Competitiveness Factors - COMPETE and National Funds through FCT - Portuguese Foundation for Science and Technology under the project Prelami PTDC/ECM/114945/2009. The first authors acknowledge the grant provided under the framework of this project.

References

[1] ACI Committee 440, *"Guide for the design and construction of externally bonded FRP systems for strengthening concrete structures"*, American Concrete Institute, 118 pp. (2002).

[2] *fib* - Bulletin 14, *"Externally bonded FRP reinforcement for RC structures"*, Technical report by Task Group 9.3 FRP (Fiber Reinforced Polymer) reinforcement for concrete structures, Féderation Internationale du Béton - *fib*, July, 130 pp. (2001).

[3] Bakis, C.E., Bank, L.C., Brown, V.L., Cosenza, E., Davalos, J.F., Lesko, J.J., Machida, A., Riskalla, S.H. and Triantafillou, T.C., *"Fiber-reinforced polymer composites for construction – state-of-the-art review"*, Journal of Composites for Construction, 6(2), pp. 73-87 (2002).

[4] Rahimi, H. and Hutchinson A., *"Concrete beams strengthened with externally bonded FRP plates"*, Journal of Composites for Construction, Volume 5, Issue 1, pp. 44-56 (2001).

[5] M.R. Esfahani, M.R. Kianoush and A.R. Tajari, *"Flexural behaviour of reinforced concrete beams strengthened by CFRP sheets"*, Engineering Structures, Volume 29, Issue 10, October, pp. 2428-2444 (2007).

[6] Barros, J.A.O., Dias, S.J.E. and Lima J.L.T., *"Efficacy of CFRP-based techniques for the flexural and shear*

strengthening of concrete beams", Journal Cement & Concrete Composites, Volume 29, Issue 3, March, pp. 203-217 (2007).

[7] Carolin, A., "*Carbon fibre reinforced polymers for strengthening of structural elements*", PhD Thesis, Division of Structural Engineering, Luleå University of Technology, Lulea, Sweden, 190 pp. (2003).

[8] El-Hacha, R. and Riskalla, S.H., "*Near-surface-mounted fiber-reinforced polymer reinforcements for flexural strengthening of concrete structures",* ACI Structural Journal, 101(5), pp. 717-726 (2004).

[9] Barros, J.A.O. and Fortes, A.S., "*Flexural strengthening of concrete beams with CFRP laminates bonded into slits*", Journal Cement and Concrete Composites, 27(4), pp. 471-480 (2005).

[10] Kotynia, R., *"Analysis of the flexural response of NSM FRP-strengthened concrete beams"*, 8th International Symposium on Fiber Reinforced Polymer (FRP) Reinforcement for Concrete Structures (FRPRCS-8), Patras, Greece, July 16-18 (2007).

[11] Bonaldo, E.; Barros, J.A.O. and Lourenço, P.J.B., *"Efficient strengthening technique to increase the flexural resistance of existing RC slabs"*, ASCE Composites for Construction Journal, 12(2), 149-159, March/April 2008.

[12] Dalfré, G.M. and Barros, J.A.O., *"NSM technique to increase the load carrying capacity of continuous RC slabs"*, Engineering Structures Journal, 56, 137-153, 2013.

[13] Barros, J.A.O., "Pre-stress technique for the flexural strengthening with NSM-CFRP strips", 9th International Symposium on Fiber Reinforced Polymer Reinforcement for Concrete Structures, Sydney, Australia, paper 85, 13-15 July (2009).

[14] Badawi M. and Soudki K., "*Flexural strengthening of RC beams with prestressed NSM CFRP rods - Experimental and analytical investigation"*, Construction and Building Materials Journal, 23, pp. 3292-3300 (2009).

[15] El-Hacha, R. and Gaafar M., "Flexural strengthening of reinforced concrete beams using prestressed, near-surface-mounted CFRP bars", PCI Journal, Fall 2011.

[16] Rezazadeh, M., Costa, I.G. and Barros, J.A.O., "*Influence of prestress level on NSM CFRP laminates for the flexural strengthening of RC beams*", Composite Structures Journal, Volume 116, October, pp. 489-500 (2014).

[17] Hosseini M.R.M., Dias, S.J.E. and Barros, J.A.O., *"Effectiveness of prestressed NSM CFRP laminates for the flexural strengthening of RC slabs"*, Composite Structures Journal, Volume 111, May, pp. 249-258 (2014).

[18] EN 206-1, *"Concrete - Part 1: Specification, performance, production and conformity"*, European standard, CEN, 69 pp. (2000).

[19] LNEC E397-1993, *"Concrete - Determination of the elasticity modulus under compression",* Portuguese specification from LNEC (1993).

[20] EN 10002-1, *"Metallic materials - Tensile testing. Part 1: Method of test (at ambient temperature)"*, European Standard, CEN, Brussels, Belgium, 35 pp. (1990).

[21] ISO 527-5, *"Plastics - Determination of tensile properties - Part 5: Test conditions for unidirectional fibre-reinforced plastic composites"*, International Organization for Standardization (ISO), Geneva, Switzerland, 9 pp. (1997).

[22] Costa, I.G. and Barros, J.A.O., *"Tensile creep of a structural epoxy adhesive: experimental and analytical characterization"*, International Journal of Adhesion & Adhesives, 59, 115-124, 2015.

[23] ISO 527-2, "*Plastics - Determination of tensile properties - Part 2: Test conditions for moulding and extrusion plastics*", International Organization for Standardization (1993).

[24] Costa, I.G. and Barros, J.A.O., "Design and development of hydraulic-electro-mechanical system to apply pre-stressed CFRP laminates according to the NSM technique in laboratory conditions", Technical Report no. 12-DEC/E-10, University of Minho, 59 pp, March (2012).

[25] EN 1992-1-1, "*Eurocode2: Design of Concrete Structures Parte 1-1: General Rules for Buildings*", CEN, Brussels, Belgium (2004).

[26] Barros, J.A.O., Taheri, M., Salehian, H. and Mendes P.J.D., "*A design model for fibre reinforced concrete beams pre-stressed with steel and FRP bars*", Composite Structures, 94, pp. 2494-2512 (2012).

[27] Barros, J.A.O., Oliveira, J.T., Lourenço, P.J.B. and Bonaldo, E., "*Flexural behavior of reinforced masonry panels*", ACI Structural Journal, 103(3), May, pp. 418-426 (2006).

[28] CEB-FIP Model Code. Comite Euro-International du Beton, Bulletin d'Information nº 213/214, 1993.

FIGURES AND TABLES

List of Figures:

Fig. 3 - Test set up.

Fig. 4 - Positions of the: a) displacement transducers (LVDTs); b) strain gauges in the monitored longitudinal tensile bars; c) strain gauges in the NSM CFRP laminates of non-prestressed slab; d) strain gauges in the NSM CFRP laminates of prestressed slabs (dimensions in mm).

Fig. 5 - Application of the prestress in the NSM CFRP laminates.

Fig. 6 - Strains in the CFRP *vs*. time after releasing the prestress load in S2L-20 and S2L-40 slabs: a) after 24 hours; and b) after seven days.

Fig. 7 - Force *vs.* deflection at mid-span of the tested RC slabs.

Fig. 8 - Crack patterns of the tested RC slabs.

Fig. 9 - Failure modes of the tested RC slabs.

Fig. 10 - (a) Load *vs.* strain in CFRP laminate (SG-L2, Fig. 4); (b) Load *vs.* strain in tensile steel reinforcement (SG-S2, Fig. 4).

Fig. 11 - Effect of the prestress level on cracking, service, yielding and ultimate loads of the RC slabs.

Fig. 12 - Effect of the prestress level on yielding and ultimate deflection of the RC slabs.

Fig. 13 - Effect of increasing the prestress level on the ductility of the RC slabs.

Fig. 14 - Influence of the concrete strength in the effectiveness of the prestressed NSM CFRP laminates.

Fig. 15 - Concrete laws used in the numerical simulations: (a) in compression [26]; (b) in tension [9].

Fig. 16 - Stress-strain relationship for the steel bars [9].

Fig. 17 - Experimental *vs.* numerical force-deflection at mid-span for the tested RC slabs: a) SREF, b) S2L-0, c) S2L-20, d) S2L-40.

Fig. 18 - Cross-section of the RC slabs strengthened with prestressed NSM CFRP laminates (parametric study): a) effect of the CFRP percentage; b) effect of the percentage of tensile longitudinal bars.

Fig. 19 - RC slabs strengthened with prestressed NSM CFRP laminates: effect of the CFRP percentage.

Fig. 20 - Effectiveness of NSM technique with prestressed CFRP laminates *vs* percentage of the CFRP.

Fig. 21 - RC slabs strengthened with prestressed NSM CFRP laminates: effect of the percentage of tensile longitudinal bars.

Fig. 22 - Effectiveness of NSM technique with prestressed CFRP laminates *vs* percentage of tensile longitudinal bars.

Fig. 23 - RC slabs strengthened with prestressed NSM CFRP laminates: effect of the elasticity modulus of the CFRP laminates.

Fig. 24 - Effectiveness of NSM technique with prestressed CFRP laminates *vs* elasticity modulus of the FRP laminates.

List of Tables:

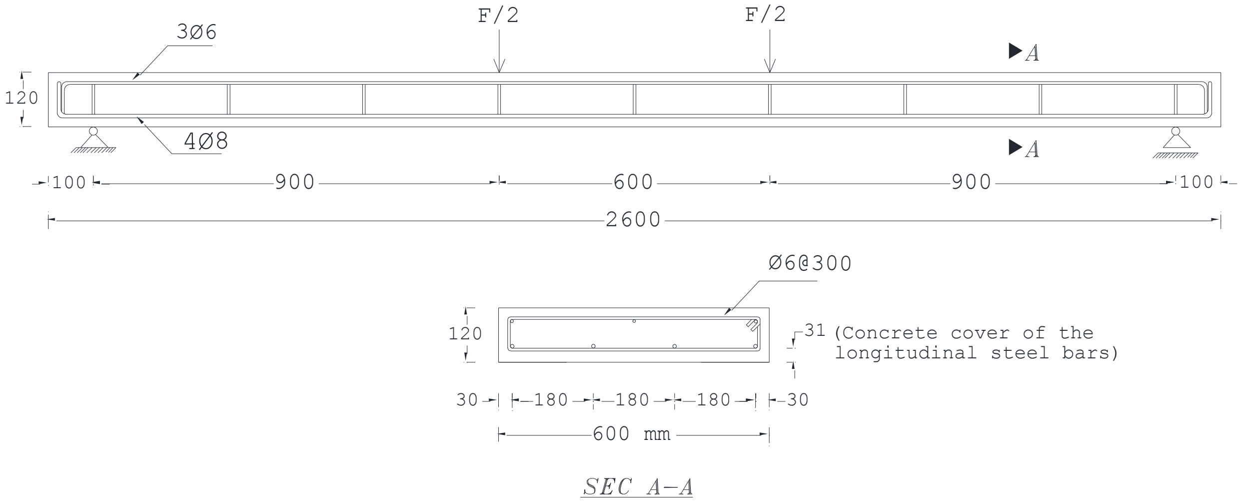

Fig. 1 - General information about the tested RC slabs (dimensions in mm).

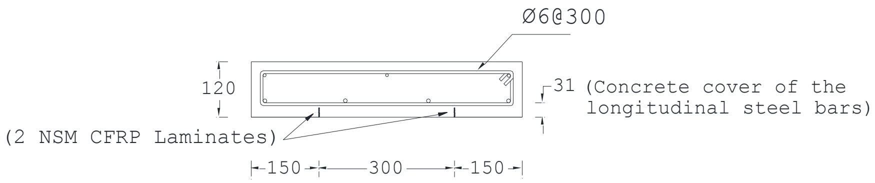

Fig. 2 - Cross-section of the RC slabs strengthened with NSM CFRP laminates (dimensions in mm).

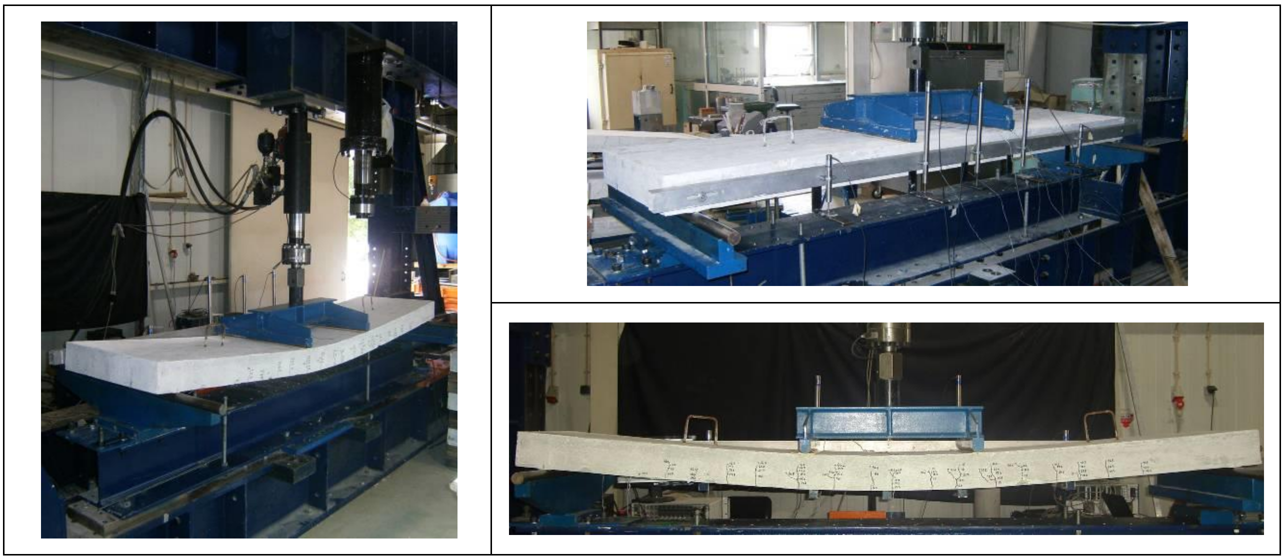

Fig. 3 - Test setup.

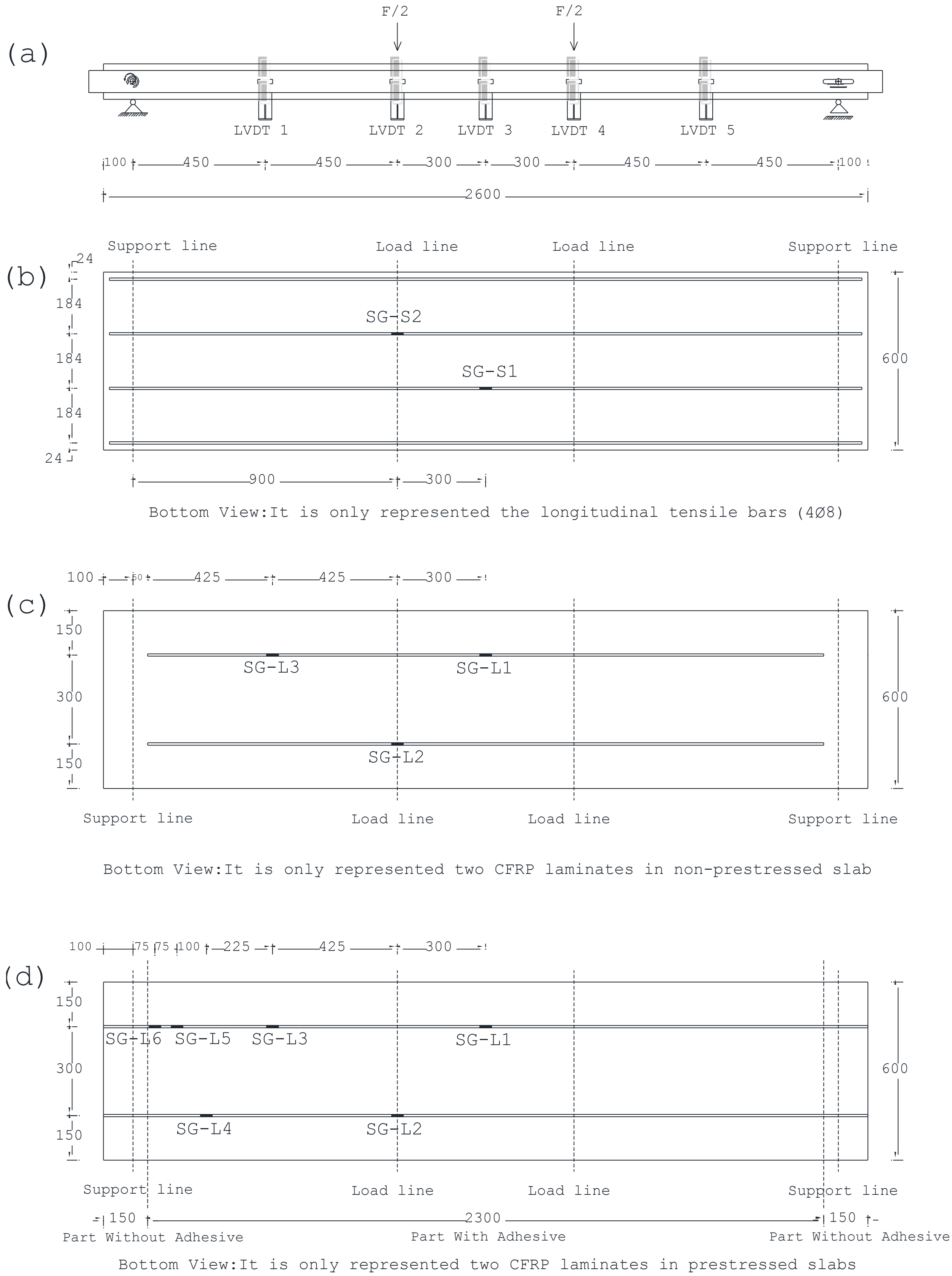

Fig. 4 - Positions of the: a) displacement transducers (LVDTs); b) strain gauges in the monitored longitudinal tensile bars; c) strain gauges in the NSM CFRP laminates of non-prestressed slab; d) strain gauges in the NSM CFRP laminates of prestressed slabs (dimensions in mm).

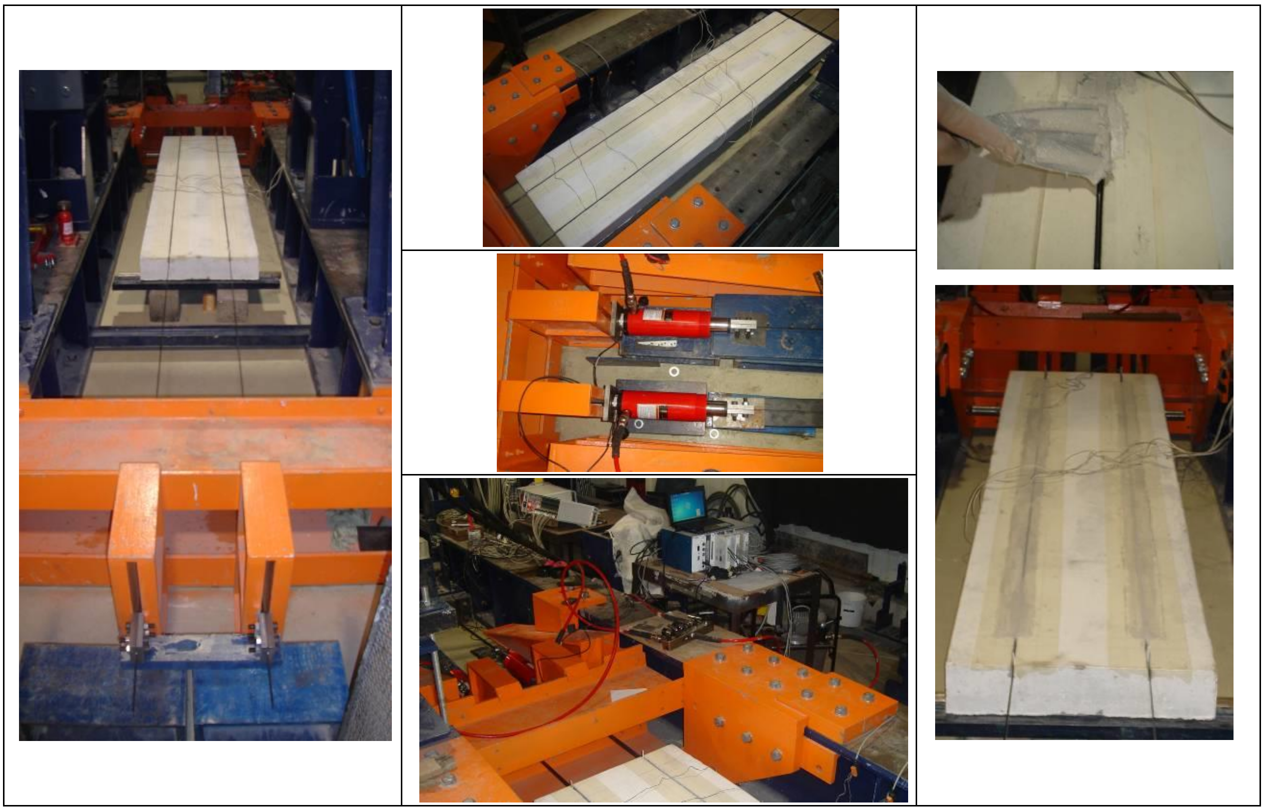

Fig. 5 - Application of the prestress in the NSM CFRP laminates.

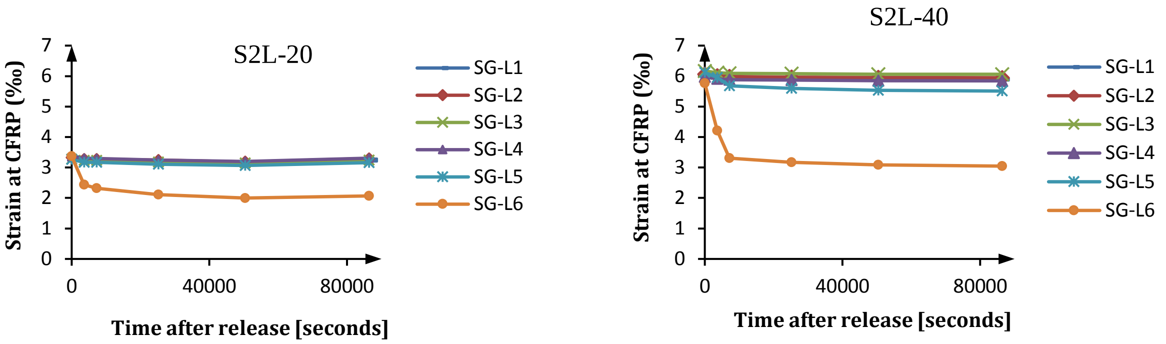

a)

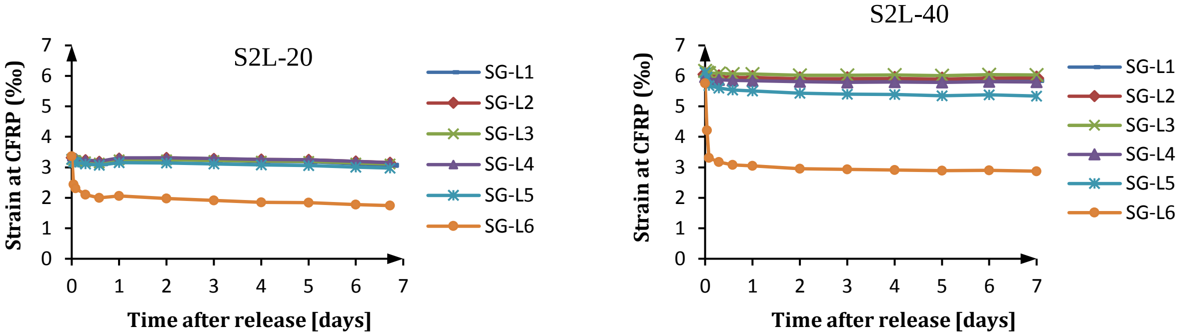

b)

Fig. 6 - Strains in the CFRP *vs*. time after releasing the prestress load in S2L-20 and S2L-40 slabs: a) after 24 hours; and b) after seven days.

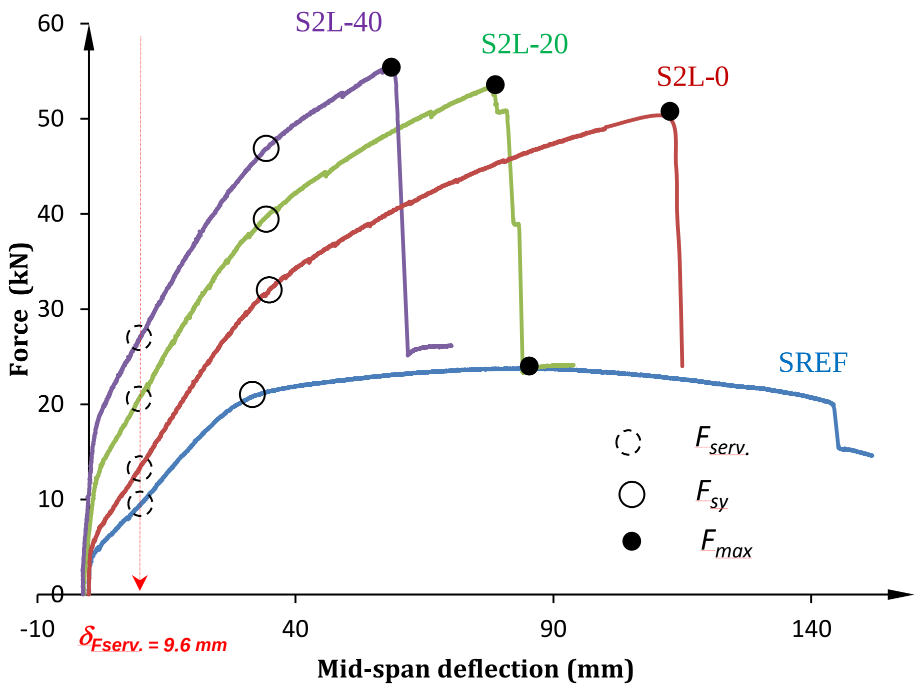

Fig. 7 - Force *vs.* deflection at mid-span of the tested RC slabs.

Non-strengthened RC slab (SREF slab)

RC slab strengthened with non-prestressed CFRP laminates (S2L-0 slab)

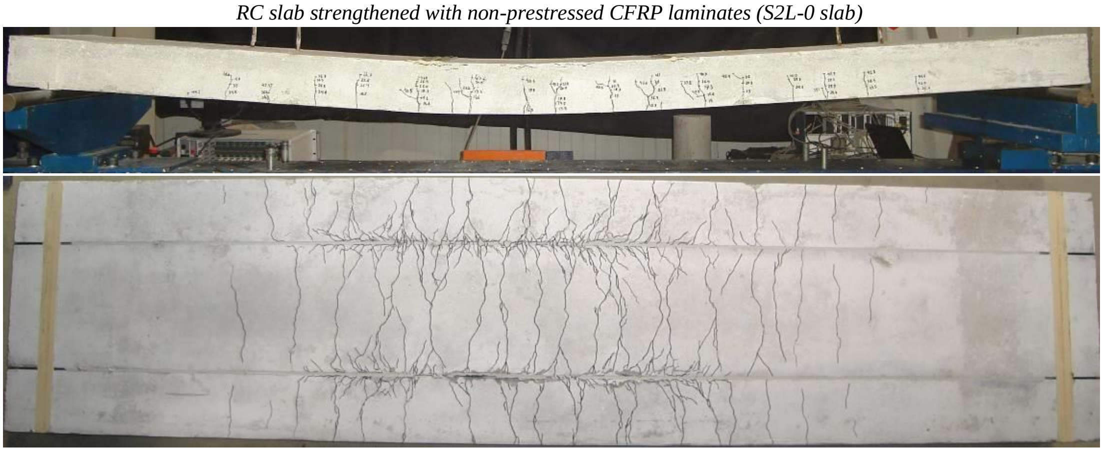

RC slab strengthened with prestressed CFRP laminates - 20% (S2L-20 slab)

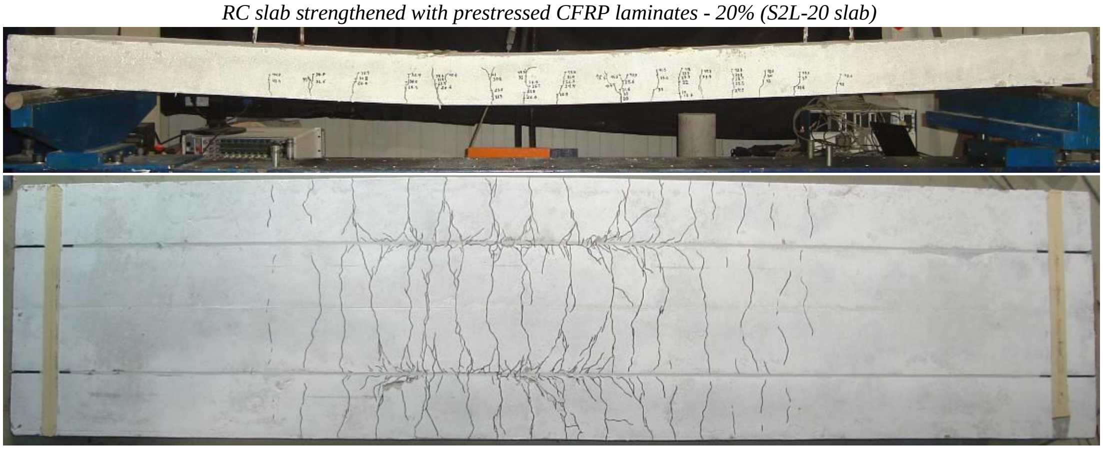

RC slab strengthened with prestressed CFRP laminates - 40% (S2L-40 slab)

Fig. 8 - Crack patterns of the tested RC slabs.

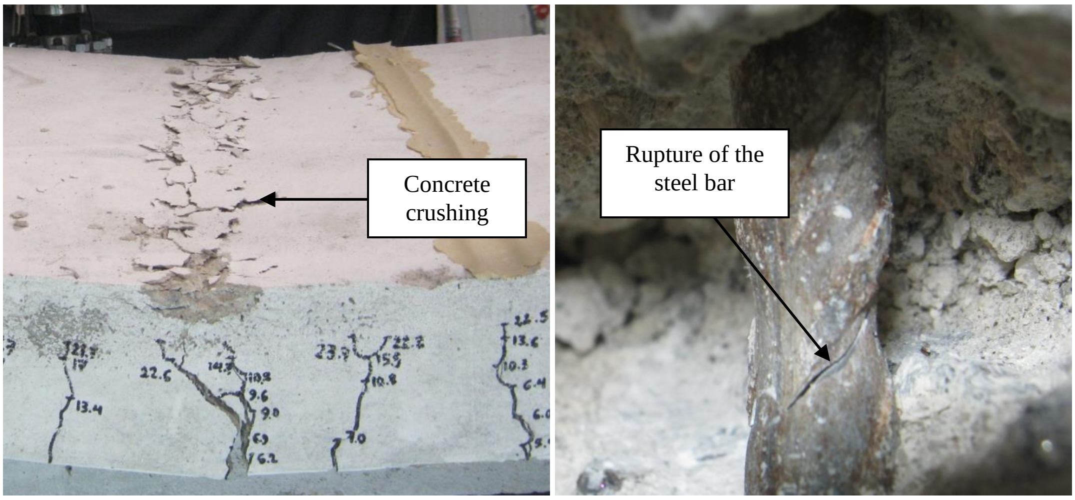

a) Concrete crushing and tensile rupture of a steel bar in the reference RC slab

b) Rupture of the CFRP in the slabs strengthened with NSM CFRP laminates

Fig. 9 - Failure modes of the tested RC slabs.

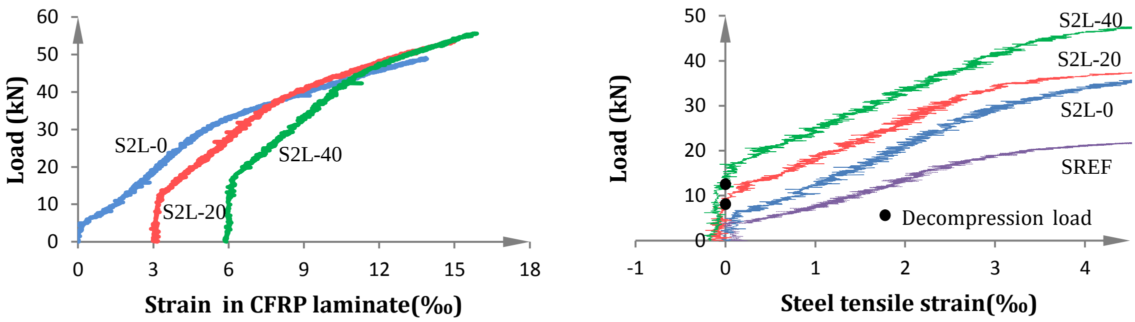

(a) (b)

Fig. 10 - (a) Load *vs.* strain in CFRP laminate (SG-L2, Fig. 4); (b) Load *vs.* strain in tensile steel reinforcement (SG-S2, Fig. 4).

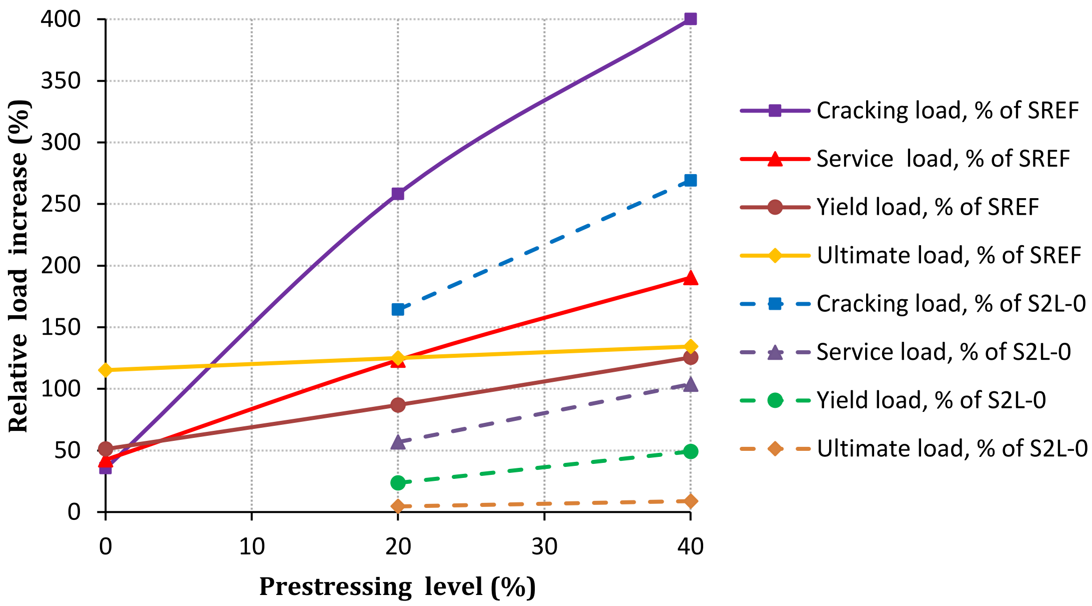

Fig. 11 - Effect of the prestress level on cracking, service, yielding and ultimate loads of the RC slabs.

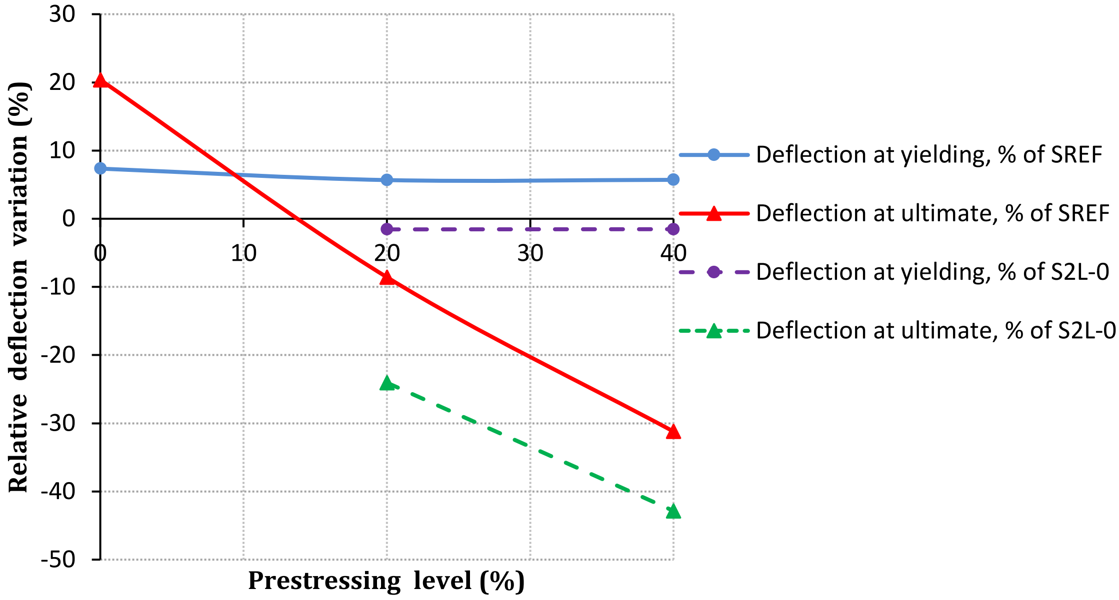

Fig. 12 - Effect of the prestress level on yielding and ultimate deflection of the RC slabs.

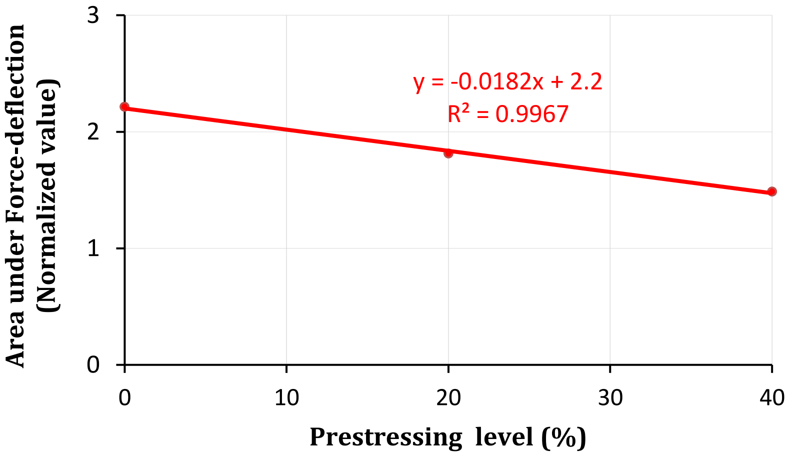

Fig. 13 - Effect of increasing the prestress level on the ductility of the RC slabs.

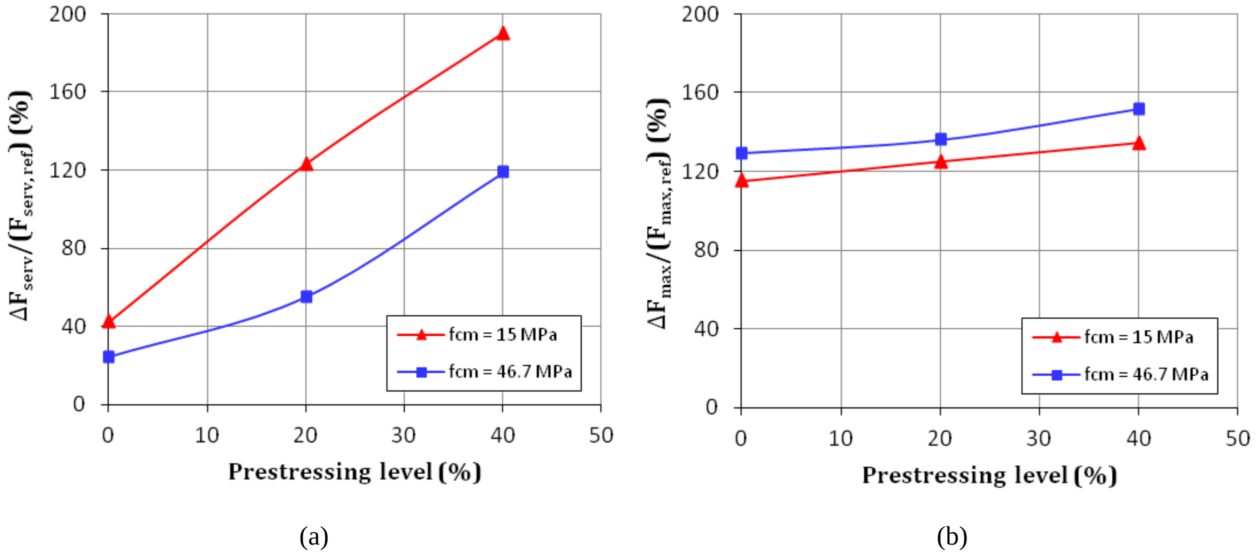

Fig. 14 - Influence of the concrete strength in the effectiveness of the prestressed NSM CFRP laminates.

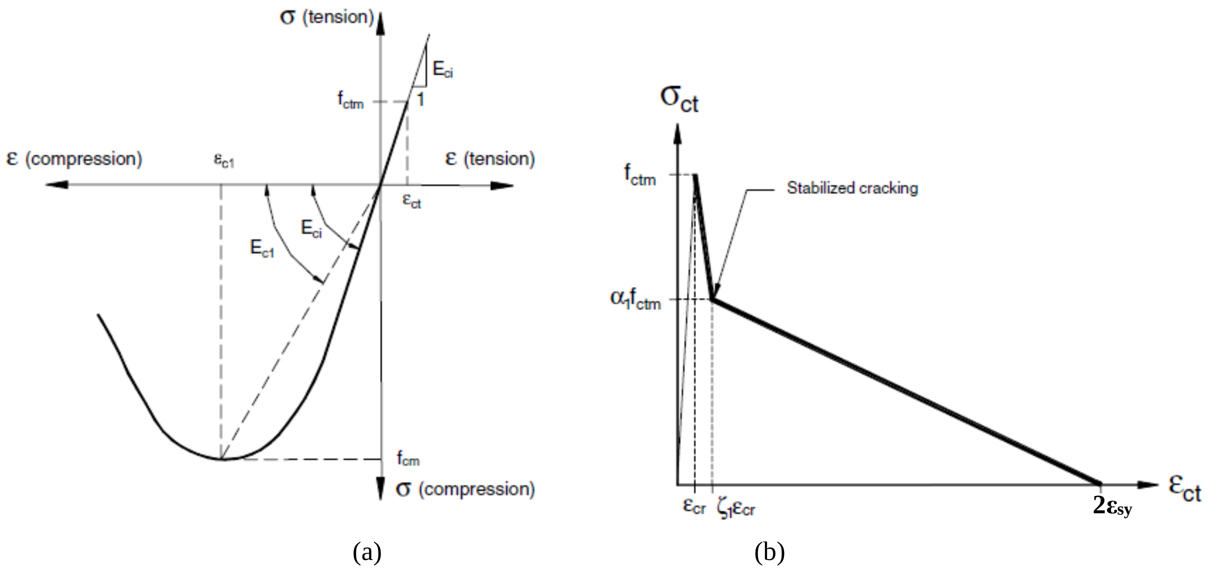

Fig. 15 - Concrete laws used in the numerical simulations: (a) in compression [26]; (b) in tension [9].

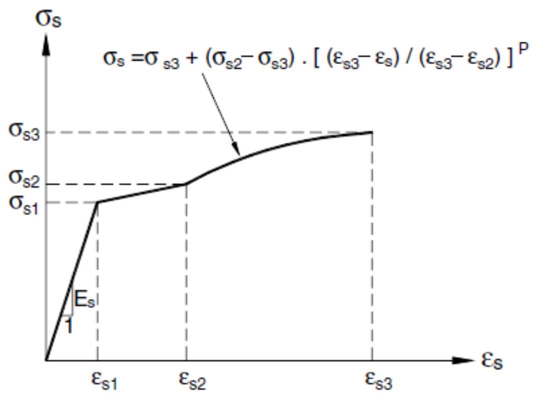

Fig. 16 - Stress-strain relationship for the steel bars [9].

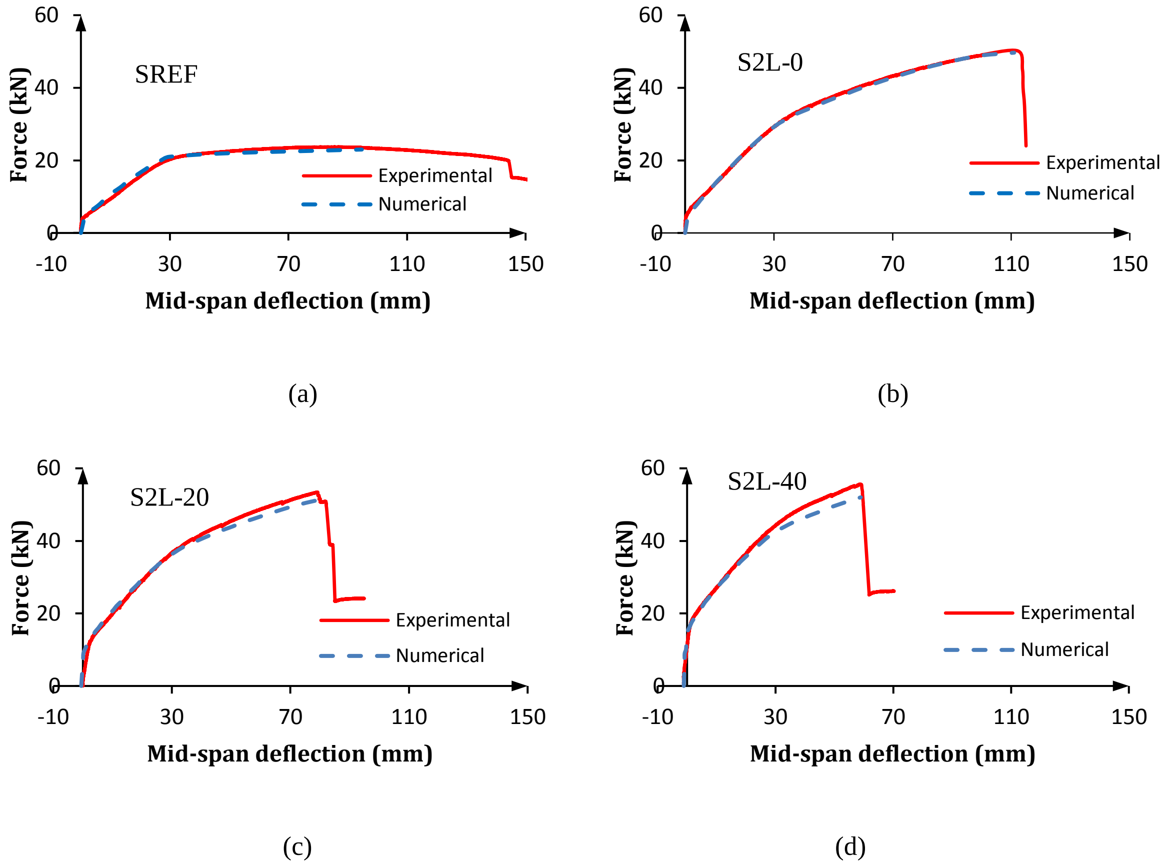

Fig. 17 - Experimental *vs.* numerical force-deflection at mid-span for the tested RC slabs: a) SREF, b) S2L-0, c) S2L-20, d) S2L-40.

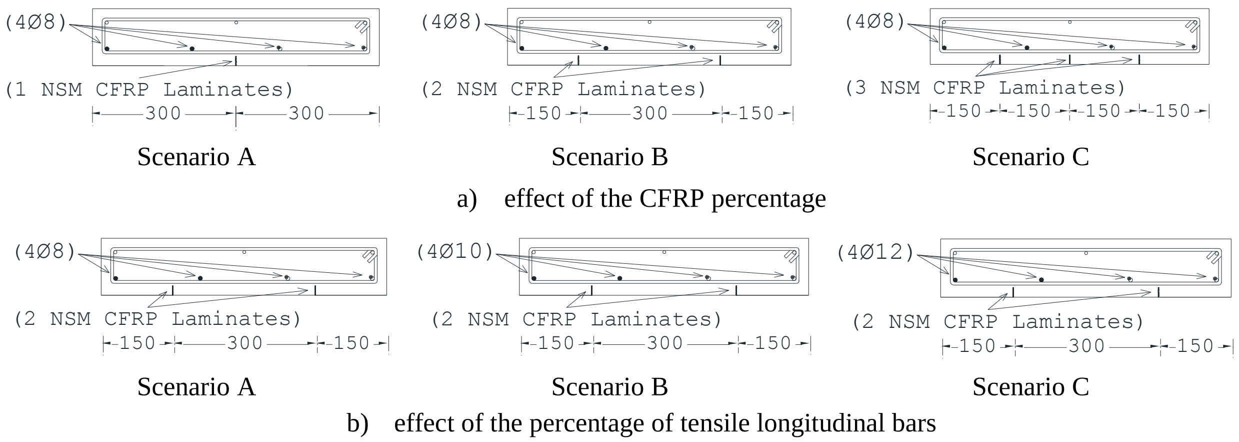

Fig. 18 - Cross-section of the RC slabs strengthened with prestressed NSM CFRP laminates (parametric study): a) effect of the CFRP percentage; b) effect of the percentage of tensile longitudinal bars.

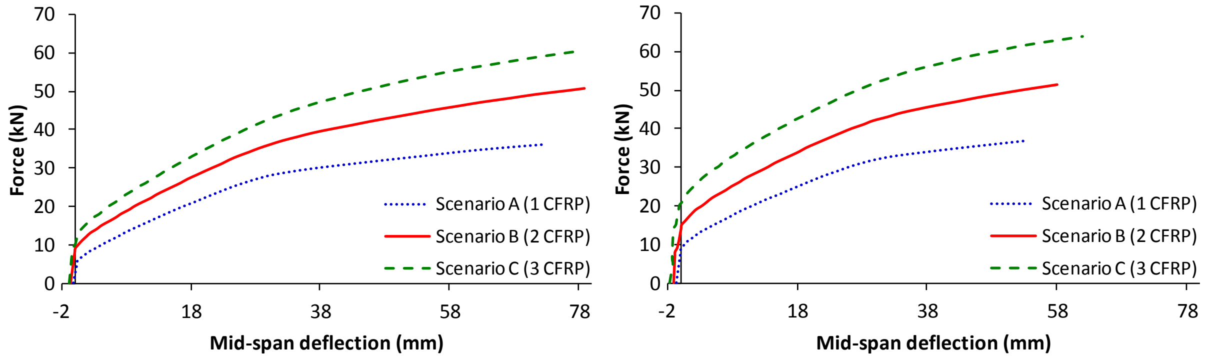

a) 20% of prestressed b) 40% of prestressed

Fig. 19 - RC slabs strengthened with prestressed NSM CFRP laminates: effect of the CFRP percentage.

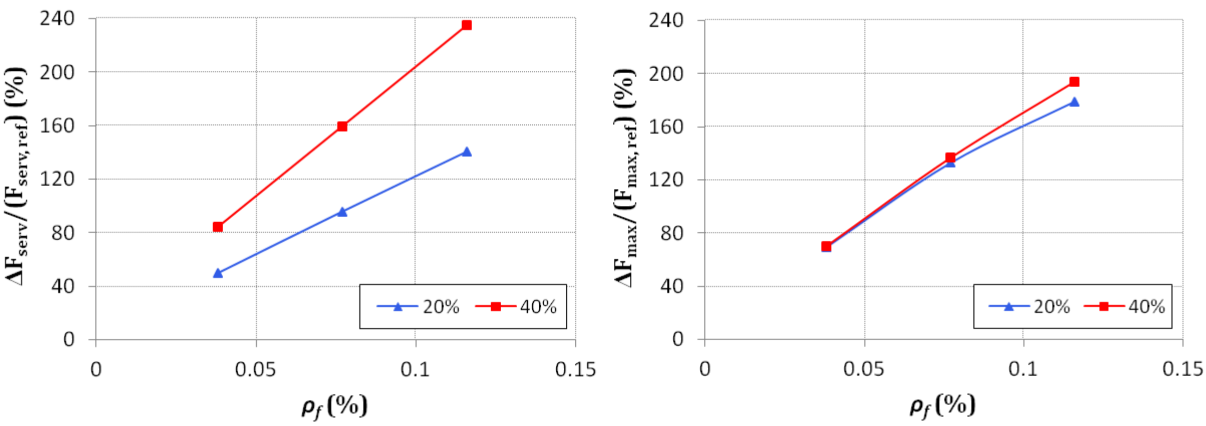

a) service load b) maximum load

Fig. 20 - Effectiveness of NSM technique with prestressed CFRP laminates *vs* percentage of the CFRP.

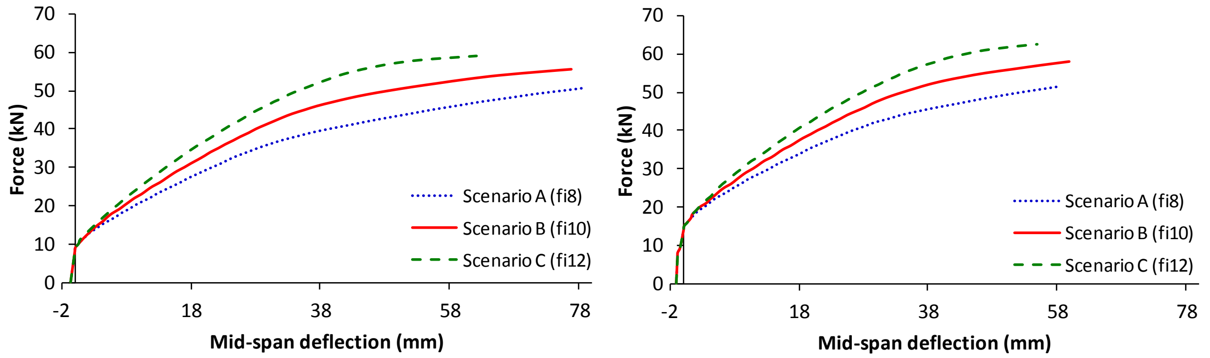

a) 20% of prestressed b) 40% of prestressed

Fig. 21 - RC slabs strengthened with prestressed NSM CFRP laminates: effect of the percentage of tensile longitudinal bars.

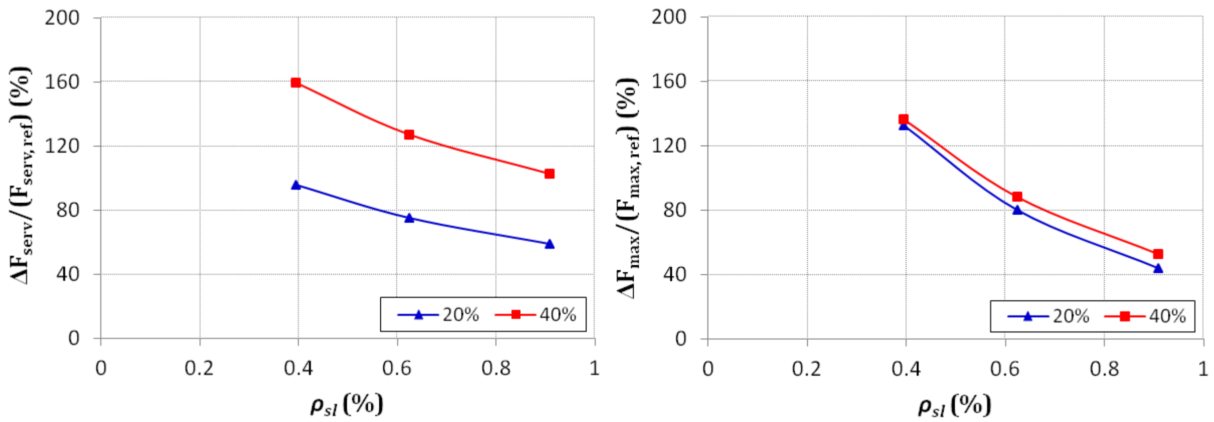

a) service load b) maximum load

Fig. 22 - Effectiveness of NSM technique with prestressed CFRP laminates *vs* percentage of tensile longitudinal bars.

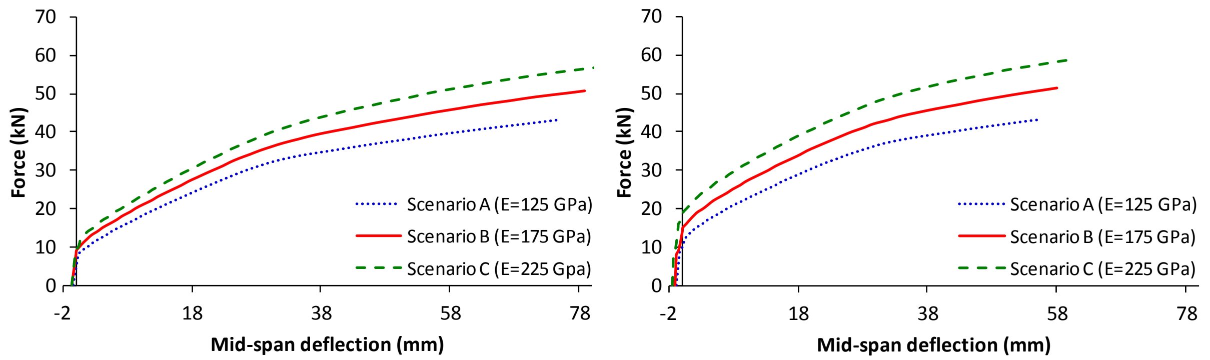

a) 20% of prestressed b) 40% of prestressed

Fig. 23 - RC slabs strengthened with prestressed NSM FRP laminates: effect of the elasticity modulus of the FRP laminates.

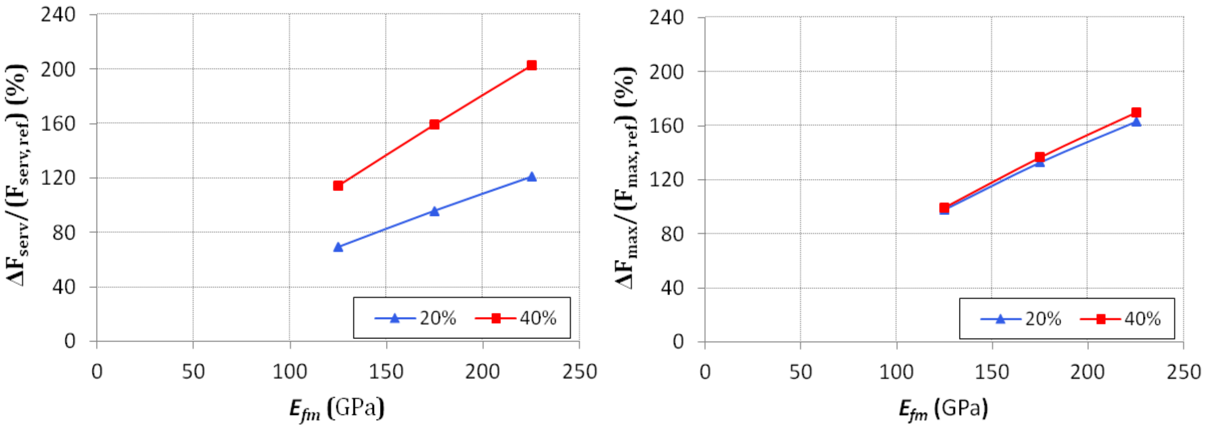

a) service load b) maximum load

Fig. 24 - Effectiveness of NSM technique with prestressed CFRP laminates *vs* elasticity modulus of the FRP laminates.

Table 1 - General information of the tested RC slabs.

Slab	ρ_{sl} (%) [(1)]	NSM CFRP flexural strengthening		Level of prestress (%)
		Quantity	ρ_f (%) [(2)]	
SREF	0.394	-	-	-
S2L-0		2 CFRP laminates with 1.4×20 mm^2 of cross section (A_f = 2×1.4×20 = 56 mm^2)	0.077	0
S2L-20				20
S2L-40				40

(1) The percentage of the longitudinal tensile reinforcement was obtained from $\rho_{sl} = \left(A_{sl}/\left(b_w \times d\right)\right)\times 100$, where A_{sl} is the cross sectional area of the longitudinal tensile steel reinforcement (see Fig. 1), b_w = 600 mm is the width of the slab's cross section, and d is the distance from extreme compression fibre to the centroid of tensile reinforcement. (2) The CFRP percentage was obtained from $\rho_f = \left(A_f / A_c\right)\times 100$, where A_f is the cross sectional area of the NSM CFRP laminates and A_c is the concrete cross sectional area.

Table 2 - Values of the properties of intervening materials.

Concrete	Compressive strength	Young´s modulus	
	f_{cm} = 15.0 MPa (at 336 days - age of slab tests)	E_{cm} = 25.0 GPa (at 336 days - age of slab tests)	
Steel	Tensile strength	ϕ6	ϕ8
	f_{sym} (yield stress)	527.6 MPa	556.4 MPa
	f_{sum} (tensile strength)	651.4 MPa	679.9 MPa
CFRP Laminates	Tensile strength	Elasticity modulus	Maximum strain
	f_{fum} = 2770.1 MPa	E_{fm} = 175.7 GPa	ε_{fu} = 15.8 ‰

Table 3 - Values of loss of strain in S2L-20 and S2L-40 slabs.

Slab	Days after releasing	Strain loss (%)					
		SG-L1	SG-L2	SG-L3	SG-L4	SG-L5	SG-L6
S2L-20	1	2.21	0.88	0.89	1.14	3.22	38.74
	2	1.94	0.53	0.89	1.14	3.67	41.25
	3	2.74	1.33	1.34	1.76	4.56	43.25
	4	3.89	1.94	2.06	2.72	5.55	44.90
	5	4.06	2.30	2.51	3.00	6.09	45.24
	6	6.18	3.80	4.03	4.65	7.70	47.23
	7	7.42	5.04	5.01	5.88	8.77	48.19
S2L-40	1	1.82	1.80	1.72	2.17	9.95	47.13
	2	2.46	2.43	2.34	2.71	11.20	48.70
	3	2.51	2.48	2.43	3.01	11.77	49.16
	4	2.51	2.33	2.24	2.91	11.87	49.36
	5	2.90	2.63	2.58	3.10	12.49	49.87
	6	2.26	2.19	1.96	2.71	12.11	49.67
	7	2.51	2.19	2.24	2.91	12.73	50.12

Table 4 - Summary of the results in terms of loads and deflections.

Slab	Cracking	Service	Yielding		Maximum	
	F_{crack} (kN)	$F_{serv.}$ (kN)	F_{sy} (kN)	u_{Fsy} (mm)	F_{max} (kN)	u_{Fmax} (mm)
SREF	3.10	9.20	21.10	29.80	23.75	85.50
S2L-0	4.20	13.10	31.80	31.99	51.11	102.92
S2L-20	11.10	20.54	40.00	31.49	53.44	78.17
S2L-40	15.50	26.70	45.85	31.50	55.65	58.82

Table 5 - Maximum strain values recorded in CFRP laminates's strain gauges up to the maximum load of the slabs.

Slab	SG-L1 (‰)			SG-L2 (‰)			SG-L3 (‰)		
	Prestressing	Test	Total	Prestressing	Test	Total	Prestressing	Test	Total
S2L-0	-	14.55	14.55	-	14.57	14.57	-	4.74	4.74
S2L-20	3.07	11.87	14.94	3.16	11.80	14.96	3.11	3.99	7.10
S2L-40	5.85	9.05	14.90	5.92	9.87	15.79	6.02	2.90	8.92

Table 6 - Performance of the NSM technique by considering relevant results of the strengthened and reference slabs.

Slab	$\Delta F_{cr}/F_{cr}^{ref}$ (%)	$\Delta F_{serv}/F_{ser}^{ref}$ (%)	$\Delta F_{max}/F_{max}^{ref}$ (%)	$\Delta u_{F_{max}}/u_{F_{max}}^{ref}$ (%)
S2L-0	35	42	115	20.
S2L-20	258	123	125	-9
S2L-40	400	190	134	-31

Table 7 - Influence of the concrete strength in the effectiveness of the prestressed NSM CFRP laminates.

Level of prestress (%)	$\Delta F_{serv}/F_{ser}^{ref}$ (%)		$\Delta F_{max}/F_{max}^{ref}$ (%)		$\Delta u_{F_{max}}/u_{F_{max}}^{ref}$ (%)	
	f_{cm} = 15 MPa	f_{cm} = 46.7 MPa	f_{cm} = 15 MPa	f_{cm} = 46.7 MPa	f_{cm} = 15 MPa	f_{cm} = 46.7 MPa
0%	42	24	115	129	20	-46
20%	123	55	125	136	-9	-60
40%	190	119	134	152	-31	-73

Table 8 - Properties of the steel bars used in the numerical simulation.

Bar diameter (mm)	E_s (GPa)	ε_{s1} (mm/mm)	σ_{s1} (MPa)	ε_{s2} (mm/mm)	σ_{s2} (MPa)	ε_{s3} (mm/mm)	σ_{s3} (MPa)	P
6, 8	190	0.003	589	0.03	620	0.15	680	3

Table 9 - Parameters evaluated in the parametric study.

Level of prestress	Percentage of the CFRP, ρ_f (%)			Percentage of tensile longitudinal bars (ρ_{sl})			Elasticity modulus of the CFRP, E_f (GPa)		
	A	B[(1)]	C	A[(1)]	B	C	A	B[(1)]	C
20%	0.038	0.077	0.116	0.394	0.623	0.908	125	175	225
40%									

[(1)] The values for this scenario are the values obtained in section 5.1 for the slabs tested in the experimental program described in this paper.

Table 10 - RC slabs strengthened with prestressed NSM CFRP laminates: effect of the CFRP percentage.

Prestress level	Scenario	CFRP laminates	ρ_f (%)	F_{serv} (kN)	F_{max} (kN)	$\Delta F_{serv}/F_{ser}^{ref}$ (%) [(1)]	$\Delta F_{max}/F_{max}^{ref}$ (%) [(1)]	u_{Fmax} (mm)
20%	A	1	0.038	15.47	36.86	50.19	69.78	73.00
	B	2	0.077	20.18	50.58	95.92	132.98	79.00
	C	3	0.116	24.76	60.55	140.39	178.91	78.70
40%	A	1	0.038	19.00	37.00	84.47	70.43	53.14
	B	2	0.077	26.75	51.37	159.71	136.62	58.00
	C	3	0.116	34.51	63.75	235.05	193.64	62.00

[(1)] The values of F_{serv}^{Ref} and F_{max}^{Ref} obtained in numerical simulation for the reference RC slab were respectively 10.3 kN and 21.71 kN.

Table 11 - RC slabs strengthened with prestressed NSM CFRP laminates: effect of the percentage of tensile longitudinal bars.

Prestress level	Scenario	Tensile longitudinal bars	ρ_{sl} (%)	F_{serv} (kN)	F_{max} (kN)	$\Delta F_{serv}/F_{ser}^{ref}$ (%)	$\Delta F_{max}/F_{max}^{ref}$ (%)	u_{Fmax} (mm)
20%	A [(1)]	4ϕ8	0.394	20.18	50.58	95.92	132.98	79.00
	B [(2)]	4ϕ10	0.623	22.22	55.61	75.37	80.49	76.90
	C [(3)]	4ϕ12	0.908	24.14	59.06	59.13	44.33	62.12
40%	A [(1)]	4ϕ8	0.394	26.75	51.37	159.71	136.62	58.00
	B [(2)]	4ϕ10	0.623	28.8	58.03	127.31	88.35	60.00
	C [(3)]	4ϕ12	0.908	30.73	62.56	102.58	52.88	55.00

[(1)] The values of F_{serv}^{Ref} and F_{max}^{Ref} obtained in numerical simulation for the reference RC slab were respectively 10.3 kN and 21.71 kN.
[(2)] The values of F_{serv}^{Ref} and F_{max}^{Ref} obtained in numerical simulation for the reference RC slab were respectively 12.67 kN and 30.81 kN.
[(3)] The values of F_{serv}^{Ref} and F_{max}^{Ref} obtained in numerical simulation for the reference RC slab were respectively 15.17 kN and 40.92 kN.

Table 12 - RC slabs strengthened with prestressed NSM CFRP laminates: effect of the elasticity modulus of the CFRP laminates.

Prestress level	Scenario	Elasticity modulus of the CFRP (GPa)	$F_{serv.}$ (kN)	F_{max} (kN)	$\Delta F_{serv}/F_{ser}^{ref}$ (%) [(1)]	$\Delta F_{max}/F_{max}^{ref}$ (%) [(1)]	u_{Fmax} (mm)
20%	A	125	17.43	43.00	69.22	98.07	74.49
	B	175	20.18	50.58	95.92	132.98	79.00
	C	225	22.74	57.10	120.78	163.01	82.00
40%	A	125	22.10	43.22	114.56	99.08	55.00
	B	175	26.75	51.37	159.71	136.62	58.00
	C	225	31.20	58.61	202.91	169.97	60.00

[(1)] The values of F_{serv}^{Ref} and F_{max}^{Ref} obtained in numerical simulation for the reference RC slab were respectively 10.3 kN and 21.71 kN.